Arabian Journal of Chemistry (2021) **14**, 102931

King Saud University

**Arabian Journal of Chemistry**

www.ksu.edu.sa
www.sciencedirect.com

ORIGINAL ARTICLE

# Green synthesis of gold nanoparticles using aqueous extract of *Mentha Longifolia* leaf and investigation of its anti-human breast carcinoma properties in the *in vitro* condition

**Shuiqin Li [a,b], Fahad A. Al-Misned [c], Hamed A. El-Serehy [c], Linlin Yang [d,*]**

[a] *Department of Rehabilitation Medicine, The First Affiliated Hospital of Xi'an Medical University, No.48 Fenghao West Road, Lianhu District, Xi'an, Shaanxi 710077, China*
[b] *Xi'an Jiaotong University, No.28 Xianning West Road, Beilin District, Xi'an, Shaanxi 710049, China*
[c] *Department of Zoology, College of Science, King Saud University, Riyadh 11451, Saudi Arabia*
[d] *Department of Hematology and Rheumatology, Central Hospital Affiliated to Shandong First Medical University, No. 105 Jiefang Road, Jinan City, Shandong Province, 250000, China*

Received 26 August 2020; accepted 3 December 2020
Available online 13 December 2020

**KEYWORDS**

Gold NPs;
*Mentha Longifolia* leaf;
Green synthesis;
Human breast cancer

**Abstract** In this research, we reported an environment friendly approach for the synthesis of gold nanoparticles (Au NPs) using *Mentha Longifolia* leaf extract. The formation of the Au NPs was characterized by UV–visible and FT-IR spectroscopy, XRD, SEM, EDX and TEM analyses. The UV–Visible spectra of gold nanoparticles showed a surface plasmon resonance peak at 512 nm. The crystalline nature of gold nanoparticles was stablished by XRD diffraction pattern. TEM revealed the spherical shape with a mean particle size of 36.4 nm. Thereafter, biological performance of those biomolecule functionalized Au NPs was investigated. To survey the anti-human breast cancer effects of gold nanoparticles, MTT assay was used on the common breast cancer cell lines i.e., breast adenocarcinoma (MCF7), breast carcinoma (Hs 578Bst), breast infiltrating ductal cell carcinoma (Hs 319.T), and breast infiltrating lobular carcinoma (UACC-3133). The conversion was achieved in short reaction time with good to excellent yields in association with outstanding turnover frequency (TOF). In addition, the nanocomposite catalyst was easily recovered and recycled for 12 successive times without noticeable decrease in catalytic activity. Gold nanoparticles had high anti-breast cancer activities dose-dependently against MCF7, Hs 578Bst, Hs 319.T, and UACC-3133 cell lines. The best result of anti-breast cancer effects was seen in the case of the

* Corresponding author.
E-mail address: yyasas6677@sina.com (L. Yang).
Peer review under responsibility of King Saud University.

Production and hosting by Elsevier

https://doi.org/10.1016/j.arabjc.2020.102931

UACC-3133 cell line. It looks gold nanoparticles can be used for the treatment of several types of breast cancers in human.



## 1. Introduction

Gold nanoparticles (Au NPs) have attracted wide attention due to their potential applications in catalysis, electrical conductivity, optical properties, etc. (Ranjith and Matijevic, 1998; Liu and Corma, 2018; Hamers, 2017; Hutchison, 2016; Gao et al., 2019; Wang et al., 2019). These can be readily synthesized and display high chemical as well as thermal stability (Son and Bao, 2018; Naseri et al., 2018; Zhang et al., 2019). Although various physical and chemical routes have been approved for the synthesis of Au NPs, such methods are not considered environmentally friendly which limited their applications in food and medical fields (Hu et al., 2017; Sharma et al., 2015; Shen et al., 2016; Antonyraj et al., 2013). In recent years, the development of efficient green chemistry methods for the synthesis of Au NPs has become a major focus of researchers. One of the methods is the production of Au NPs using biological system such as microbes, fungi and plant extracts (Menon et al., 2017; Yazdankhah et al., 2018; Xia et al., 2013; Anastas and Eghbali, 2010; Anastas and Kirchhoff, 2002; Clark, 2002; Hutchison, 2008). Plant mediated synthesis of Au NPs are noteworthy due to its simplicity, rapid rate of synthesis, eco-friendliness and it can potentially render more biocompatibility with biomolecules (Varma, 2014).

The major advantage of using extracts is that they are the mild, renewable and non-toxic reducing and stabilizing agents, eliminating the need for chemical reducing agents such as sodium borohydride and expensive polymeric capping agents and stabilizers. (Mohammadinejad et al., 2016; Machado et al., 2013; Lopez-Tellez et al., 2013; Kumar et al., 2013; Kharissova et al., 2013; Sharma et al., 2019). In the recent days, this green metric protocol for the synthesis of noble metal NPs has been quite popular (Nadagouda et al., 2014; Sarmah et al., 2019; Vishnukumar et al., 2017; Sun et al., 2014) and ample studies are going on for the biogenic synthesis of Au nanoparticles (Choudhary et al., 2017; Vimalraj et al., 2018; Panichikkal et al., 2019; Khan et al., 2018; Dong et al., 2015; Annamalai et al., 2013). Au NPs find extensive applications in diverse fields like biological transmission electron microscopy, colorimetric DNA sensors based on colloidal Au and catalysis (Suchomel et al., 2018). One of their therapeutic properties is anti-cancer especially anti-breast cancer properties (Katata-Seru et al., 2018; Sangami and Manu, 2017; Beheshtkhoo et al., 2018).

Breast cancer is the main cancer between all women in all of the world. It is caused in the breast tissue and after a while distributed to all of the body through metastasis (Bray et al., 2018). The metastatic carcinoma, inflammatory carcinoma of the breast, infiltrating lobular carcinoma of breast, infiltrating ductal cell carcinoma, breast carcinoma, and breast adenocarcinoma are five main types of breast cancer (Bray et al., 2018; Boyd et al., 2007). The main symptoms of breast cancer are lump in a breast, red scaly patch of skin, fluid coming from the nipple, a newly inverted nipple, dimpling of the skin, and change in breast shape (Bray et al., 2018; Boyd et al., 2007; Siu, 2016). For the treatment of breast cancer, surgery, radiation therapy, chemotherapy, targeted therapy, immunotherapy, and EGFR-targeted therapy are used (Jahanzeb, 2008). The main anti-breast cancer chemotherapeutic drugs are included cyclophosphamide, doxorubicin, taxane, docetaxel, methotrexate, trastuzumab, pertuzumab, and fluorouracil (Bray et al., 2018; Jahanzeb, 2008). According to the high side effects of chemotherapeutic drugs such as nausea, fatigue, hair loss, vomiting, diarrhea, weight loss, and mouth sores, the formulation of modern chemotherapeutic drugs is necessary (Moschini et al., 2016). Recently, scientists have understood that metallic nanoparticles especially gold nanoparticles have excellent anticancer properties (Hemmati et al., 2019).

The *Mentha Longifolia* plant have been used as a crucial anti-hypertensive drug and anti-tussive, expectorant in traditional chinese medicine (Namvar et al., 2014; Kaneko et al., 1981). The main constituents of this plant include polyphenols, alkaloids, organic acids, terpenoids, carbohydates and *etc.* (Badfar-Chaleshtori et al., 2012). Now, based on the research on the biosynthesis of metal NPs (Bhat et al., 2005; Shahriary et al., 2018; Jalalvand et al., 2019; Abay et al., 2017; Wu et al., 2019), we report herein the green synthesis of Au NPs using *Mentha Longifolia* leaf extract for the first time. The as synthesized Au NPs were characterized with analytical techniques like UV–visible Spectroscopy, Fourier Transformed Infrared Spectroscopy (FT-IR), Scanning Electron Microscopy (SEM), Transmission Electron Microscopy (TEM), Energy Dispersive X-ray spectroscopy (EDX) and Powder X-ray diffraction (XRD). Next, we decided to investigate the anti-breast cancer potentials of gold nanoparticles formulated by *Mentha Longifolia* leaf against breast adenocarcinoma, breast carcinoma, breast infiltrating ductal cell carcinoma, and breast infiltrating lobular carcinoma cell lines.

## 2. Experimental

### 2.1. Materials and apparatus

All the reagents were purchased from Aldrich and Merck and were used without any purification. The crystalline structures of the samples were evaluated by X-ray diffraction (XRD) analysis on a Bruker D8 Advance diffractometer with CuK$\alpha$ radiation at 40 kV and 20 mA. Fourier transform infrared (FT-IR) spectra were recorded using KBr pellet with a Perkin Elmer 65 spectrometer in the range of 400–4000 $cm^{-1}$. TEM images at the accelerating voltage of 80 KV were taken with a Zeiss -EM10C. Morphology and particle dispersion was investigated by field emission scanning electron microscopy (FESEM) (Cam scan MV2300). The chemical composition of the prepared nanostructures was measured by EDS (Energy Dispersive X-ray Spectroscopy) performed in SEM. The

UV–Vis absorbance spectra were recorded using double beam UV–Visible spectrophotometer (PG Instrument, T80 + ), equipped with 10 mm quartz cuvettes.

### 2.2. Preparation of Mentha Longifolia leaf extract

Fresh *Mentha Longifolia* leaf were collected from the Xi'an Medical University of China and washed thoroughly with double-distilled water. 2.0 g of the *Mentha Longifolia* leaf was heated in 100 mL deionized water for 30 min at 80 °C. The colored mixture was then cooled and filtered through hatmann filter paper No. 1 to have the aqueous extract. It was stored at 4 ℃ in refrigerator for further use (Hemmati et al., 2019).

### 2.3. Green synthesis of Au NPs using Mentha Longifolia leaf extract

In a typical synthesis of Au NPs, 10 mL of the aqueous extract of *Mentha Longifolia* leaf was added dropwise to 50 mL of well-mixed 0.001 M aqueous solution of $HAuCl_4$ with constant stirring at room temperature. After 20 min, the light yellow colored mixture changed to wine red, an evidence for the preparation of Au NPs (Fig. 1). Then the solution containing nanoparticles was centrifuged at 4000 rpm for 20 min and the upper transparent layer was decanted off. The residues obtained were washed for several times with deionized water and finally dried in an oven at 50℃ (Hemmati et al., 2019).

### 2.4. Measurement of the anti-human breast cancer effects of Au NPs

In this experiment, the following cell lines have been used for investigating the anti-human breast cancer effects of the $HAuCl_4$, *Mentha Longifolia* leaf, and Au NPs using an MTT assay:

(1) Breast adenocarcinoma (MCF7) with ATCC NO. HTB-22™.
(2) Breast carcinoma (Hs 578Bst) with ATCC NO. HTB-125™.
(3) Breast infiltrating ductal cell carcinoma (Hs 319.T) with ATCC NO. CRL-7236™.
(4) Breast infiltrating lobular carcinoma (UACC-3133) with ATCC NO. CRL-2988™.

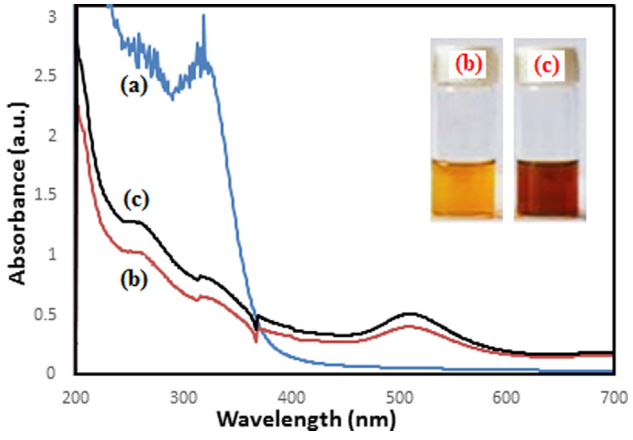


**Fig. 1** UV–vis spectrum of green synthesized Au NPs using aqueous extract of *Mentha Longifolia* during 20 min. UV–vis spectrum of extract (a); after 10 min (b) and after 20 min (c).

They were then cultured as a monolayer culture in 90% RPMI-1640 medium and 10% fetal serum and supplemented with 200 mg/mL streptomycin, 125 mg/mL penicillin, and 8 mg/mL amphotericin B. The culture was then exposed to 0.5 atmospheric carbon dioxide at 37 °C, on which the tests were performed after at least ten successful passages. MTT assay a method used to investigate the toxic effects of various materials on various cell lines, including non-cancer and cancer cells. To evaluate the cell toxicity effects of the compounds used in this research, the cells were transferred from the T25 flask to the 96-well flasks. In each cell of the 96-cell flasks, 7000 cells of cancer and fibroblast cell lines were cultured, and the volume of each cell was eventually increased to 100 µL. Before the treatment of the cells in the 96-well flak, the density of cells was increased to 70%, so the 96-well flasks were incubated for 24 h to obtain the cell density of $7 \times 10^3$. Next, the initial culture medium was discarded, and variable concentrations (0–1000 µg/mL) of $HAuCl_4$, *Mentha Longifolia* leaf, and Au NPs were incubated at 37 °C and 0.5 $CO_2$ for 24, 48, and 72 h. Then, 20 µL MTT was added to each well after a certain amount of time. Next, 100 µL DMSO solvent was added to each well. They were then kept at room temperature for 25 min and read at 490 and 630 nm by a microtitre plate reader.

The cell lines were treated with the hydroalcoholic extract (1.25 mg/mL), which inhibited about 20% of the cell growth. Annexin/PI method was used to determine the apoptosis level in the treated and control cell lines using a flow cytometry machine. To perform experiment, the cell lines were treated with a variable concentrations (0–1000 µg/mL) of $HAuCl_4$, *Mentha Longifolia* leaf, and Au NPs for 24 h. Cells were irrigated with phosphate-buffered saline (PBS). After centrifugation, buffer binding was added to the obtained precipitate. Then, 5 µL Annexin V dye was added and incubated for 15 min at 25 °C. Cells were washed with the binding solution, following which 10 µL PI dye was added. Finally, cell analysis was done by a flow cytometry machine according to the below formula (Jalalvand et al., 2019):

$$\text{Cell viability } (\%) = \frac{\text{Sample A.}}{\textit{Control A.}} \times 100$$

### 2.5. Statistical analysis

The obtained results were analyzed by SPSS (version 20) software using one-way ANOVA, followed by Duncan post-hoc test ($P \leq 0.01$).

## 3. Results and discussion

### 3.1. Characterizations of biosynthesized Au NPs

Au NPs formation was monitored visually and by UV–visible spectroscopy. The instant the *Mentha Longifolia* leaf extract was added into the aqueous solution of $HAuCl_4$, color of the solution started changing from yellow to dark red (Fig. 1,

inset). Moreover, the UV spectrum of extract (Fig. 1a) shows specified signals of phenolics inside the plants as the bands at $\lambda_{max}$ 330 nm (band I) due to the transition localized within the ring of cinnamoyl system; whereas the band around 240 nm (band II) is for absorbance of ring related to the $\pi \rightarrow \pi^*$ transitions of benzoyl system [51a]. Therefore, these absorbance bands confirm the presence of phenolics and ability of plant extract for green synthesis of nanoparticles. The reaction of Au nanoparticles was completed after 20 min following the formation of nanoparticles monitored by UV–vis spectroscopy, Fig. 1b,c. The Au NPs showed a characteristic peak centered at 512 nm indicating the surface plasmon absorption of nanosized Au particles and formation of nanoparticles.

For more convenience the FT-IR analysis was carried out to demonstrate the responsible phytochemicals during the green synthesized of Au NPs. The FT-IR spectrum of the crude extract, (Fig. 2a) depicted some peaks at 3402 $cm^{-1}$, 2872 $cm^{-1}$, 1679 $cm^{-1}$ and 1380 $cm^{-1}$ which represent free OH in molecule and OH group forming hydrogen bonds, saturated hydrocarbons ($C_{sp3}$–H), carbonyl group (C = O) and stretching C = C aromatic ring, respectively. Because of presence these functional groups inside the structure of antioxidant polyphenolics, the spectrum can demonstrate the presence of phenolics in the plant extract and support the results of related literatures (Nasrollahzadeh and Sajadi, 2015). Furthermore, FT-IR spectrum of Au NPs is shown in Fig. 2b. The appeared bands are lattice vibrational modes indicating the functional groups of biomolecules adsorbed on nanoparticles. The broad band in 3496 $cm^{-1}$ is –OH stretching bond of hydroxyl functional group. The band around 1682 $cm^{-1}$ is generally attributed to the carbonyl functional group (Yazdankhah et al., 2018).

The surface morphology of *Mentha Longifolia* extract-synthesized Au NPs was analyzed by SEM and TEM. SEM micrographs of Au NPs showed spherical shapes (Fig. 3). Moreover, particle size was evaluated by TEM analysis.

Transmission electron microscopy (TEM) has been used to identify the size and shape of nanoparticles. Typical TEM images obtained for biosynthesized Au NPs are shown in Fig. 4. From the images, it is clear that the morphology of gold nanoparticles is almost spherical. This result is in agreement with the shape of SPR bands centered at 512 nm of Au NPs (Choudhary et al., 2017). The histogram describing the size distribution of particles are shown in (Fig. 4, inset). From

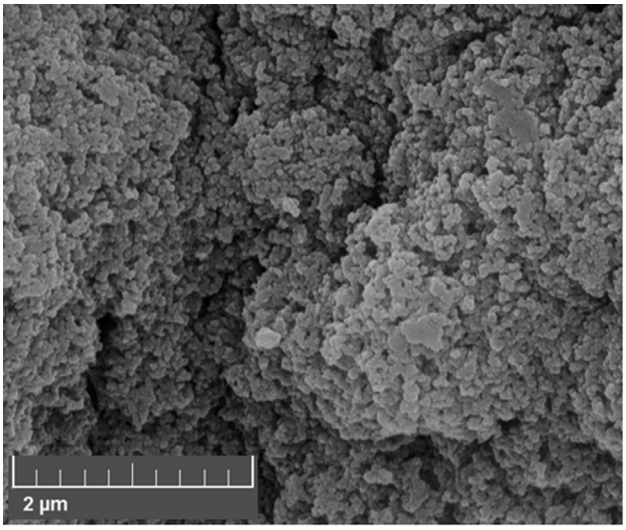


**Fig. 3** FE-SEM image of biosynthesized Au NPs.

the histogram the average particle size measured for the golid nanoparticles is observed to be 36.4 nm.

Energy Dispersive X-ray Spectroscopy (EDX) confirmed the existence of Au particles in the specimen (Fig. 5). The presence of C, N and O elements justifies the phytochemical functionalization over Au NPs.

The X-ray diffraction (XRD) profile of biosynthesized Au NPs using the *Mentha Longifolia* leaf extract is depicted in Fig. 6. It Shows intensive characteristic peaks of metallic Au. The diffraction

Peaks at 2θ 38.12°, 44.52°, 64.52° and 77.12° correspond to the (1 1 1), (2 0 0), (2 2 0) and (3 1 1) Bragg planes of *fcc* gold lattice, respectively, which are in agreement with the diffraction standard of Gold (JCPDS80-3697).

### 3.2. Anti-human breast cancer potentials of gold nanoparticles

In this study, the treated cells with several concentrations of the present $HAuCl_4$, *Mentha Longifolia* leaf extract, and Au NPs were examined by MTT test for 48 h regarding the cytotoxicity properties on normal (HUVEC), breast adenocarcinoma (MCF7), breast carcinoma (Hs 578Bst), breast

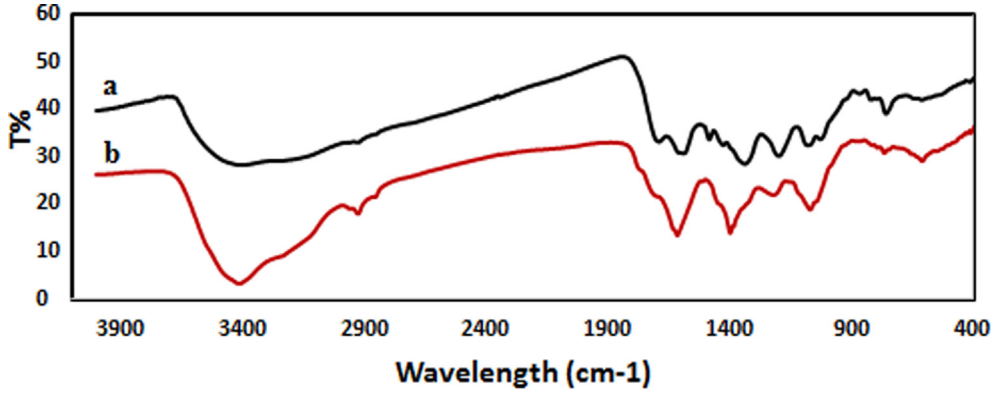


**Fig. 2** FT-IR spectra of (a) *Mentha Longifolia* leaf extract and (b) biosynthesized Au NPs.

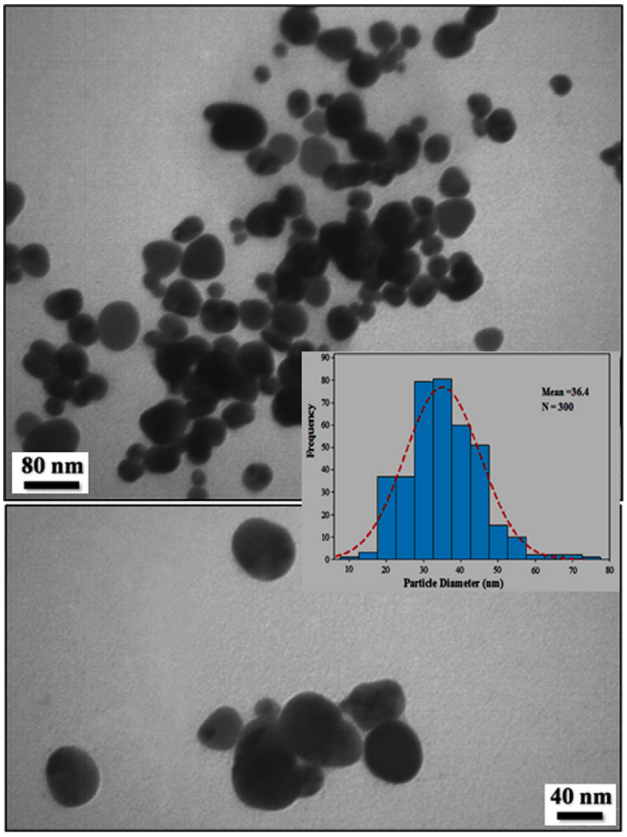


**Fig. 4** TEM images of biosynthesized Au NPs.

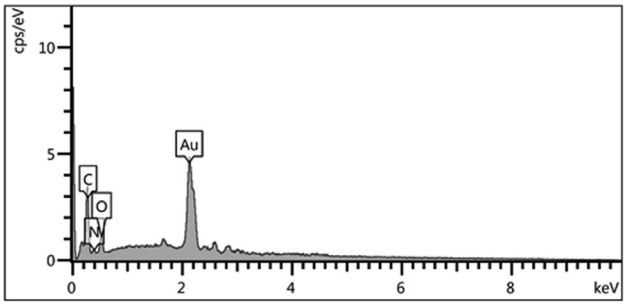


**Fig. 5** EDX spectrum of biosynthesized Au NPs.

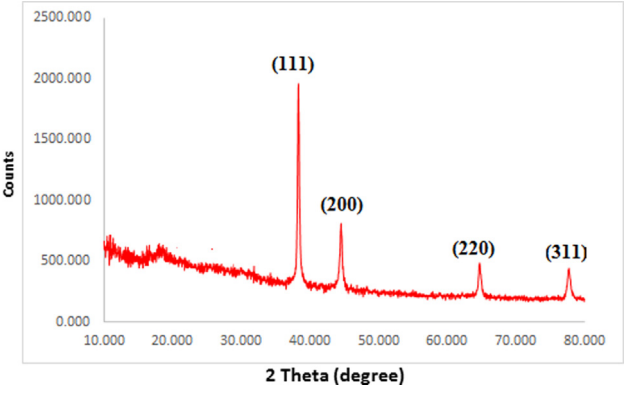


**Fig. 6** XRD pattern of biosynthesized Au NPs.

infiltrating ductal cell carcinoma (Hs 319.T), and breast infiltrating lobular carcinoma (UACC-3133) cell lines (Fig. 7,8; Table 1). The absorbance rate was determined at 570 nm, which indicated extraordinary viability on normal cell line (HUVEC) even up to 1000 μg/mL for $HAuCl_4$, *Mentha Longifolia* leaf extract, and Au NPs.Fig. 8.

In the case of breast adenocarcinoma, breast carcinoma, breast infiltrating ductal cell carcinoma, and breast infiltrating lobular carcinoma cell lines, the viability of them reduced dose-dependently in the presence of $HAuCl_4$, *Mentha Longifolia* extract, and Au NPs. The IC50 of *Mentha Longifolia* and Au NPs against MCF7 cell line were 439 and 274 μg/mL, respectively; against Hs 578Bst cell line were 464 and 279 μg/mL, respectively; against Hs 319.T cell line was 418 and 274 μg/mL, respectively; and against UACC-3133 cell line were 374 and 201 μg/mL, respectively.

The best result of cytotoxicity property of gold nanoparticles against the above cell lines was seen in the case of the UACC-3133 cell line.

In the previous study, Hemmati et al. (2020) indicated that gold nanoparticles had significant efficacy on removing the acute leukemia cell lines without any cytotoxicity effect on the HUVEC cell line. In the previous study, the IC50 of gold nanoparticles were less than 200 μg/mL (Hemmati et al., 2019). In the study of Sun et al (2020), the IC50 of the gold nanoparticles were near to the 150 μg/mL against Breast cancer cell lines. Also they reported that the gold nanoparticles didn't have any cytotoxicity against HUVEC cell lines [64a].

The anticancer of gold nanoparticles was found to be highly dependent on a range of factors related to their physical characteristics, such as surface coating, shape, and size. About the size, it has been reported that gold nanoparticles with small size can transfer of cell membrane of tumor cells and remove them. In the larger size, the above ability significantly is confined (Hemmati et al., 2019). As can be observed in Figs. 3 and 4 of our study, gold nanoparticles had uniform spherical morphology in range sizes of 30–45 nm. The size of gold nanoparticles in lower than 50 nm is very suitable for the killing of tumor cell lines *in vivo* and in vitro (Hemmati et al., 2019).

About the anticancer properties of gold nanoparticles, they have used for the treatment of several cancers including human lung cancer, mammary carcinoma, uterus cancer, lung epithelial cancer, Lewis lung carcinoma, colon cancer, and human glioma [64b].

Nam et al. (Devi and Bhimba, 2012) designed functionalized gold nanoparticles using dendrimers for fight cancer cells. Similarly, the silver nanoparticles synthesized by brown seaweed Ulva show good cytotoxic activity against human laryngeal cancer (Hep-2) cell line, human breast cancer (MCF 7) cell line and human colon cancer (HT 29) cell line and breast cancer line MCF-7 (Holt et al., 1994). Recently, Rajeshkumar et al. (2016) synthesized the silver nanoparticles and reported their great potential to inhibit the cell viability of liver and lung cancer cell lines The cytotoxic effect of gold nanoparticles is the result of active physicochemical interaction of gold atoms with the functional groups of intracellular proteins, as well as with the nitrogen bases and phosphate groups in DNA (Blagoi Yu et al., 1991). In previous report Sriram et al. (2010) reported that the nanoparticles acquiring anticancer properties are known for their potential ability to slow down the activities of abnormally expressed signaling proteins, such as Akt and Ras, cytokine-based therapies, DNA- or protein based vacci-

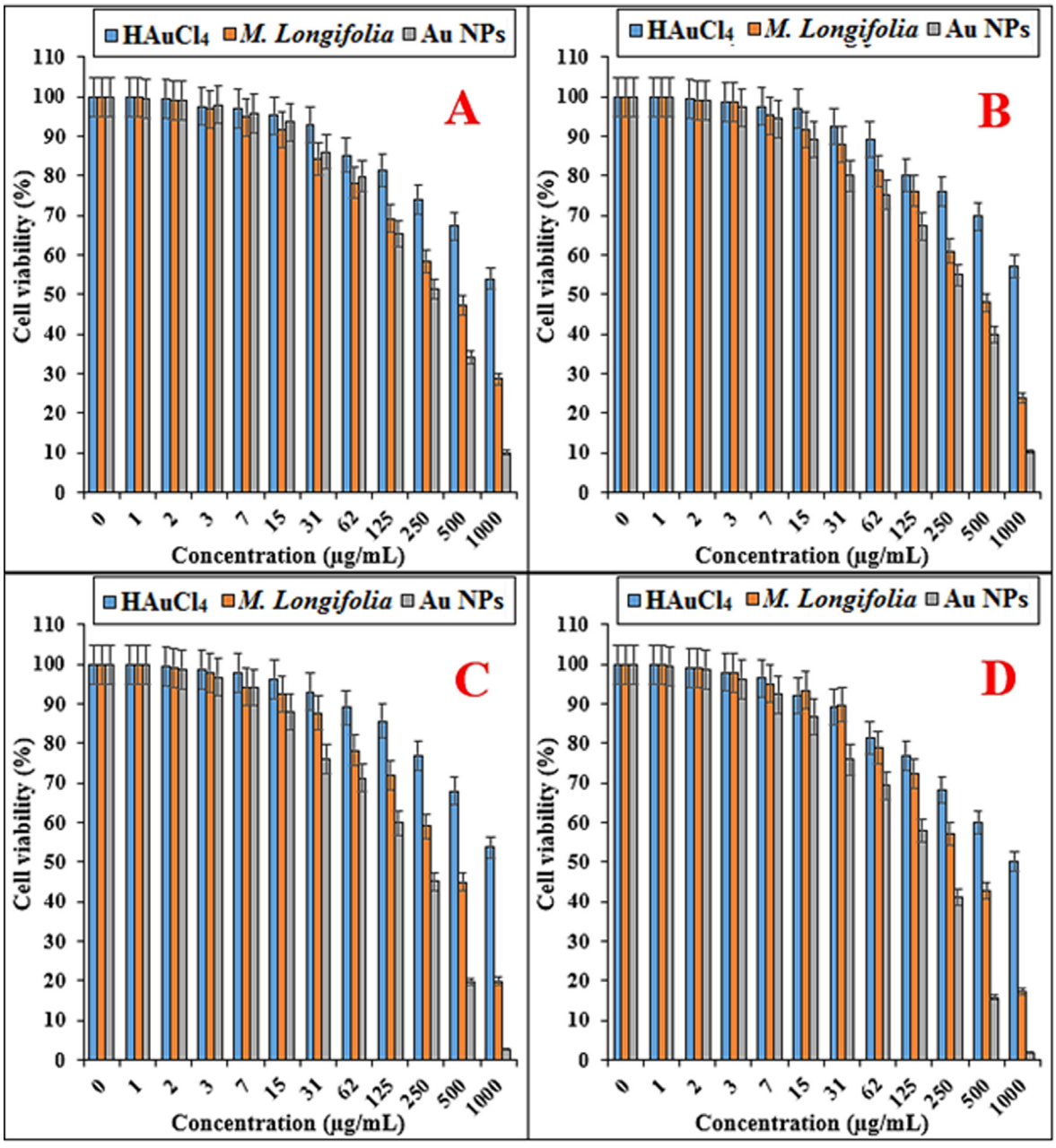


**Fig. 7** The anti-breast carcinoma properties of $HAuCl_4$, *Mentha Longifolia* leaf, and Au NPs against MCF7 (A), Hs 578Bst (B), Hs 319. T (C), and UACC-3133 (D) cell lines.

**Table 1** The IC50 of $HAuCl_4$, *Mentha Longifolia,* and Au NPs in the cytotoxicity or breast cancer test.

| | $HAuCl_4$ (µg/mL) | *M. Longifolia* (µg/mL) | Au NPs (µg/mL) |
|---|---|---|---|
| **IC50 against MCF7** | – | $439 \pm 0^a$ | $264 \pm 0^b$ |
| **IC50 against Hs 578Bst** | – | $459 \pm 0^a$ | $269 \pm 0^b$ |
| **IC50 against Hs 319.T** | – | $418 \pm 0^a$ | $224 \pm 0^b$ |
| **IC50 against UACC-3133** | – | $374 \pm 0^a$ | $201 \pm 0^b$ |

* The different words indicate the significant differences between examined groups ($P \leq 0.01$).

nes against specific tumor markers, and tyrosine kinase inhibitors which exhibit a consistent antitumor effect (Martins et al., 2010). In the previous studies, it has been indicated that the gold nanoparticles have low effects on the normal cells and its mechanism is related to the deform cell membrane of the cancer cells that allow to be identified by gold nanoparticles. In this report, the anticancer activity was observed and that the synthesized gold nanoparticles induce a dose dependent inhibition activity against breast cancer cells. Some of the approved chemotherapeutic agents were caused side effect and high cast. Therefore, there is an important need to develop alternative medicines against this deadly disease. Synthesized gold nanoparticles to fulfill the need of new therapeutic treatment were discovered.

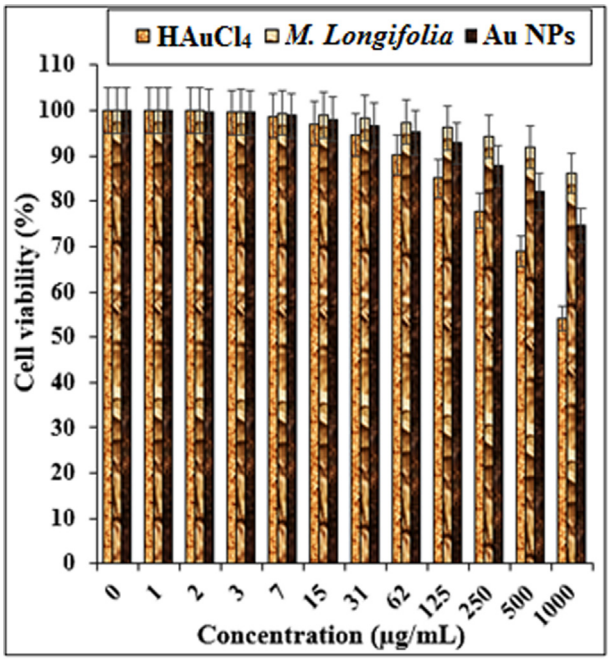


**Fig. 8** The cytotoxicity properties of $HAuCl_4$, *Mentha Longifolia,* and Au NPs against normal (HUVEC) cell line.

## 4. Conclusion

A plant-mediated, green method of synthesizing gold nanoparticles was successfully performed by employing the leaf extract of *Mentha Longifolia*. It was found out that the various biomolecules present in the leaf extract were responsible for the formation and stability of the Au NPs. The size, morphology, crystalline structure and the stability were characterized by UV–Vis spectroscopy, FT-IR, SEM, TEM, EDX and XRD analysis. The biosynthesized nanoparticles had effective anti-breast cancer effects against breast adenocarcinoma (MCF7), breast carcinoma (Hs 578Bst), breast infiltrating ductal cell carcinoma (Hs 319.T), and breast infiltrating lobular carcinoma (UACC-3133) cell lines without any cytotoxicity activity against normal cell line i.e., HUVEC. It appears that the gold nanoparticles synthesized using *Mentha Longifolia* leaf aqueous extract can be used as novel anti-breast cancer drugs in humans in the near future.

## Funding

Shaanxi Provincial Key Research and Development Plan: 2019JM-325.

## Declaration of Competing Interest

The authors declare that they have no competing interests.

## Acknowledgements

The authors extend their appreciation to the Deanship of Scientific Research at King Saud University, Riyadh, Saudi Arabia for funding this work through research group no (RG-242).

## References

Abay, A.K., Chen, X., Kuo, D.H., 2017. New J. Chem. 41, 5628–5638.
Anastas, P., Eghbali, N., 2010. Chem. Soc. Rev. 39, 301–312.
Anastas, P., Kirchhoff, M.M., 2002. Acc. Chem. Res. 35, 686–694.
Annamalai, A., Christina, V.L.P., Sudha, D., Kalpana, M., Lakshmi, P.T.V., 2013. Colloids Surf. B 108, 60–65.
Antonyraj, C.A., Jeong, J., Kim, B., Shin, S., Kim, S., Lee, K.Y., Cho, J.K., 2013. J. Ind. Eng. Chem. 19 (3), 1056–1059.
Badfar-Chaleshtori, Sajad, Shiran, Behrouz, Kohgard, Masoomeh, Mommeni, Hassan, Hafizi, Akram, Khodambashi, Mahmood, Mirakhorli, Neda, Sorkheh, Karim, 2012. Biochem. Syst. Ecol. 42, 35–48.
Beheshtkhoo, N., Kouhbanani, M.A.J., Savardashtaki, A., Amani, A. M., Taghizadeh, S., 2018. Appl. Phys. A. 124, 363–369.
(a) Bhat, S.V., Nagasampagi, B.A., Sivakumar, M., 2005. Chemistry of natural products, Narosa publishing house, New Delhi, p. 585; (b) Nasrollahzadeh, M., Sajadi, S.M., 2015. RSC Adv., 5, 46240 (c) Veisi, H., Ghorbani, M., Hemmati, S., 2019. Mater. Sci. Eng. C, , 98, 584-593; (d) Veisi, H., Moradi, S.B., Saljooqi, A., Safarimehr, P., 2019. Mater. Sci. Eng. C, 2019, 100, 445-452.
Blagoi Yu, P., Galkin, V.L., Gladchenko, G.O., Kornilova, S.V., Sorokin, V.A., Shkorbatov, A.G., 1991. Naukova Dumka, Kiev, p. 272.
Boyd, N.F., Guo, H., Martin, L.J., Sun, L., Stone, J., Fishell, E., Jong, R.A., Hislop, G., Chiarelli, A., Minkin, S., Yaffe, M.J., 2007. N. Engl. J. Med. 356, 227–236.
Bray, F., Ferlay, J., Soerjomataram, I., Siegel, R.L., Torre, L.A., Jemal, A., 2018. CA Cancer J. Clin. 68, 394–424.
Choudhary, B.C., Paul, D., Gupta, T., Tetgure, S.R., Garole, V.J., Borse, A.U., Garole, D.J., 2017. J. Environ. Sci. 55, 236–246.
Clark, J.H., 2002. Acc. Chem. Res. 35, 791–797.
Devi, J.S., Bhimba, B.V., 2012. Sci. Rep. 1 (4), 242.
Dong, B., Liu, G., Zhou, J., Wang, A., Wang, J., Jin, R., Lv, H., 2015. RSC Adv. 5, 97798–97806.
Gao, P., Pan, W., Li, N., Tang, B., 2019. ACS Appl. Mater. Interfaces 11, 26529–26558.
Hamers, R.J., 2017. Acc. Chem. Res. 50, 633–637.
Hemmati, S., Rashtiani, A., Zangeneh, M.M., Mohammadi, P., Zangeneh, A., Veisi, H., 2019. Polyhedron. 158, 8–14.
Hemmati, S., Joshani, Z., Zangeneh, A., Zangeneh, M.M., 2019. Appl. Organometal. Chem. 33,. https://doi.org/10.1002/aoc.5277 e5277.
Holt, J.G., Krieg, R.N., Sneath, P.H.A., Staley, J.T., Williams, S.T., 1994. Bergey's Manual of Determinative Bacteriology, ninth ed., Williams and Wilkins Baltimore.
Hu, M., Yao, Z., Wang, X., 2017. Ind. Eng. Chem. Res. 56, 3477–3502.
Hutchison, J.E., 2008. ACS Nano 2, 395–402.
Hutchison, J.E., 2016. ACS Sustain. Chem. Eng. 4 (11), 5907–5914.
Jahanzeb, M., 2008. Clin. Breast Cancer. 8, 324–333.
Jalalvand, A.R., Zhaleh, M., Goorani, S., Zangeneh, M.M., Seydi, N., Zangeneh, A., Moradi, R., 2019. J. Photochem. Photobiol. B. 192, 103–112.
(a) Kaneko, K., Katsuhara, T., Kitamura, Y., Nishizawa, M., Chen, Y.P., Hsu, H.Y., Chem. Pharm. Bull. 1988, 36, 4700–4705; (b) Kitajima, J., Noda, N., Ida, Y., Miyahara, K., Kawasaki, T., Heterocycles 1981, 15, 791–796.
Katata-Seru, L., Moremedi, T., Aremu, O.S., Bahadur, I., 2018. J. Mol. Liq. 256, 296–304.
Khan, M.E., Khan, M.M., Cho, M.H., 2018. RSC Adv. 8, 13898–13909.
Kharissova, O.V., Dias, H.V.R., Kharisov, B.I., Pérez, B.O., Pérez, V. M., 2013. J. Biotechnol. 31, 240–248.
Kumar, K.M., Mandal, B.K., Kumar, K.S., Reddy, P.S., Sreedhar, B., 2013. Spectrochim. Acta A 102, 128–133.
Liu, L., Corma, A., 2018. Chem. Rev. 118, 4981–5079.

Lopez-Tellez, G., Balderas-Hernandez, P., Barrera-Diaz, C.E., Vilchis-Nestor, A.R., Roa-Morales, G., Bilyeu, B., 2013. J. Nanosci. Nanotechnol. 13, 2354–2361.
Machado, S., Pinto, S.L., Grosso, J.P., Nouws, H.P.A., Albergaria, J. T., Delerue-Matos, C., 2013. Sci. Total Environ. 445, 1–8.
Martins, D., Frungillo, L., Anazzetti, M.C., Melo, P.S., Duran, N., 2010. Int. J. Nanomed. 5, 77–85.
Menon, S., Rajeshkumar, S., Venkatkumar, S., 2017. Resour.-Efficient Technol. 3, 516–527.
Mohammadinejad, R., Karimi, S., Iravani, S., Varma, R.S., 2016. Green Chem. 18, 20–52.
Moschini, M., Simone, G., Stenzl, A., Gill, I.S., Catto, J., 2016. Eur. Urol. Focus. 2, 19–29.
Nadagouda, M.N., Iyanna, N., Lalley, J., Han, C., Dionysiou, D.D., Varma, R.S., 2014. ACS Sustain. Chem. Eng. 2, 1717–1723.
Namvar, F., Rahman, H.S., Mohamad, R., Baharara, J., Mahdavi, M., Amini, E., Chartrand, M.S., Yeap, S.K., 2014. Int. J. Nanomed. 19, 2479–2488.
Naseri, N., Ajorlou, E., Asghari, F., Soltanahmadi, Y.P., 2018. Artif. Cells, Nanomed., Biotechnol. 2018, 46, 1111-1121.
Panichikkal, J., Thomas, R., John, J.C., Radhakrishnan, E.K., 2019. Curr. Microbiol. 76, 503–509.
Rajeshkumar, S., Malarkodi, C., Vanaja, M., Annadurai, G., 2016. J. Mol. Struct. 1116, 165–173.
Ranjith, D., Matijevic, E., 1998. New J. Chem. 22, 1203–1215.
Sangami, S., Manu, B., 2017. Environ. Technol. Innov. 8, 150–163.
Sarmah, M., Neog, A.B., Boruah, P.K., Das, M.R., Bharali, P., Bora, U., 2019. ACS Omega 4, 3329–5340.
(a) Shahriary, M., Veisi, H., Hekmati, M., Hemmati, S., Mater. Sci. Eng. C, 2018, 90, 57-66; (b) Veisi, H., Mirzaei, A., Mohammadi, P., 2019. RSC Adv., 9 (2019) 41581; (c) Shaham, G., Veisi, H., Hekmati, M., 2017. Appl. Organometal. Chem. 31, e3737.
Sharma, D., Kanchi, S., Bisetty, K., 2019. Arab. J. Chem. 12 (8), 3576–3600. https://doi.org/10.1016/j.arabjc.2015.11.002.
Sharma, N., Ojha, H., Bharadwaj, A., Pathak, D.P., Sharma, R.K., 2015. RSc. Adv. 5, 53381–53403.
Shen, K., Chen, X., Chen, J., Li, Y., 2016. ACS Catal. 6, 5887–5903.
Siu, A.L., 2016. Ann Intern Med. 164, 279–296.
Son, D., Bao, Z., 2018. ACS Nano 12, 11731–11739.
Sriram, M.I., ManiKanth, S.B., Kalishwaralal, K., Gurunathan, S., 2010. Int. J. Nanomed. 5, 753–762.
Suchomel, P., Kvitek, L., Prucek, R., Panacek, A., Halder, A., Vajda, S., Zboril, R., 2018. Sci. Rep. 8, 1–11.
Sun, D., Zhang, G., Jiang, X., Huang, J., Jing, X., Zheng, Y., He, J., Li, Q., 2014. J. Mater. Chem. A 2, 1767–1773.
Varma, R., 2014. Green Chem. 16, 2027–2041.
Vimalraj, S., Ashokkumar, T., Saravanan, S., 2018. Biomed. Pharmacother. 105, 440–448.
Vishnukumar, P., Vivekanandhan, S., Muthuramkumar, S., 2017. ChemBioEng. Rev. 4, 18–36.
Wang, M., Mohanty, S.K., Mahendra, S., 2019. Acc. Chem. Res. 52 (3), 876–885.
Wu, G., Liu, X., Zhou, P., Wang, L., Hegazy, M., Huang, X., Huang, Y., 2019. Mat. Sci. Eng. C. 94, 524–533.
Xia, Y., Yang, H., Campbell, C.T., 2013. Acc. Chem. Res. 46 (8), 1671–1672.
Yazdankhah, M., Veisi, H., Hemmati, S., 2018. J. Taiwan Inst. Chem. Eng. 91, 38–46.
Zhang, Q., Yang, X., Guan, J., Appl, A.C.S., 2019. Nano Mater. 2, 4681–4697.